Kinematic characterization of free-falling near-spherical droplets impacting a viscous liquid film

Yixuan Dong[1], Taoyu Pan[2], Ruicheng Li[3]

[1] Nanjing Foreign Language School, Nanjing 210000, China;

Abstract. In industrial settings, the flow characteristics of liquids are pivotal in processes such as piping, mixing, and filtration. A thorough understanding of liquid flow behavior under diverse conditions is essential for optimizing industrial processes and enhancing productivity. This paper investigates a specific fluid dynamic phenomenon: the motion of a liquid droplet interacting with a soap film. The experimental variables include droplet release height, droplet diameter, soap film inclination angle, and soapy water concentration—all of which influence the droplet's motion characteristics. During the experiments, three distinct phenomena were observed under different conditions: the droplet traversed the soap film, merged into the film, or was repelled by it. A review of the literature reveals that prior studies have primarily focused on these phenomena in isolation, overlooking the combined effects of the aforementioned experimental variables. To address this gap, this thesis proposes a surface tension model for the soap film, systematically analyzes the force balance and energy conversion mechanisms of near-spherical droplets, and derives preliminary relationships between the variables and droplet motion characteristics. Through controlled-variable experiments, the observed phenomena were found to align closely with theoretical predictions, validating the proposed theoretical model's accuracy.

Keywords: Liquid flow characteristics; Fluid dynamic phenomenon; Liquid droplet; Surface tension model.

1. Introduction

Soap bubbles, as iconic elements of childhood recreation, have transcended their role as playthings to become significant subjects in scientific inquiry. These ephemeral structures have made substantial contributions to fluid dynamics research, elucidating fundamental mechanisms of surface tension and interfacial phenomena. Plateau's pioneering work in the 19th century demonstrated how surface tension drives the minimization of the interfacial area in bubble formation. Subsequent investigations uncovered the self-restorative properties of soap films, wherein the Marangoni effect governs fluid dynamics: localized film thinning induces surface tension gradients, triggering surfactant-driven fluid transport from regions of lower to higher surface tension. This spontaneous redistribution effectively restores film integrity through viscoelastic relaxation processes.

In recent years, scholarly interest in soap bubbles has expanded to encompass more complex phenomena, including their morphological characteristics, interactions with solid spheres, and membrane rupture mechanisms. For instance, Taylor (1976) established a foundational connection between soap films and minimal surfaces, demonstrating how these films naturally approximate solutions to minimal surface problems [1]. Courant (1940) further investigated the geometric configurations of soap films and their underlying structural principles [2]. Ruckenstein, E., and Jain, R. K. (1971) systematically analyzed rupture dynamics induced by droplet-film interactions, providing a theoretical framework for film destabilization [3]. Similarly, Gilet, T., and Bush, J. W. M. (2009) advanced the understanding of film stability through experimental studies on foreign object penetration, elucidating critical factors affecting interfacial toughness [4].

However, a review of existing literature shows most studies focus on single-variable effects in experiments, neglecting multi-independent variable analysis or controlled-variable series. Limited research exists on droplet-soap film interactions, especially regarding soap film angles relative to the horizontal. To address this, we designed experiments to examine effects of droplet fall height, soap film angle, droplet size, and soapy water concentration on post-collision motion. Controlling drop height regulated impact velocity. Varying capillary tube diameters altered droplet size for penetration

analysis. Two soapy water concentrations were tested to assess concentration effects. High-speed cameras recorded interactions, with results analyzed frame-by-frame. Post-experiment, a preliminary modeling analysis of droplet-film interaction was conducted using surface tension theory and energy conservation principles.

2. Theory and Modeling

2.1 Qualitative interpretation of experimental phenomena

The interaction between a droplet and a soap film is governed by energy conservation principles. Upon collision, the soap film deforms downward, increasing its surface area and thereby elevating its surface energy. This energy gain is sourced from the droplet's kinetic energy loss, assuming negligible droplet deformation or coalescence with the film. Air resistance exerts minimal influence compared to the droplet-film interaction, allowing the system's total energy—comprising the soap film's surface energy and the droplet's mechanical energy—to remain approximately conserved. Crucially, the soap film exhibits a critical deformation threshold, beyond which rupture occurs [5]. This threshold is determined by the film's surface tension and the supporting ring's diameter. By analyzing the balance between the droplet's initial mechanical energy (primarily kinetic) and the soap film's surface energy under varying experimental conditions, the outcome of droplet-film collisions—penetration or rebound—can be systematically predicted [6].

Four key parameters govern the collision outcome: (1) Droplet Height: Elevated release heights enhance the droplet's kinetic energy upon impact, increasing the likelihood of film penetration. (2) Soap Film Inclination Angle: Tilting the film reduces the droplet's velocity component perpendicular to the film surface. A steeper angle diminishes this velocity, favoring rebound over penetration [7]. (3) Soap Concentration: Higher soap concentrations amplify surface tension, thereby raising the film's surface energy. This strengthens the film's resistance to penetration, promoting droplet rebound. (4) Droplet Size: Larger droplets possess greater initial mechanical energy, enhancing their propensity to penetrate the film. This parametric framework quantitatively links experimental variables to energy-driven collision outcomes, establishing a predictive model for dynamic droplet-film interactions.

2.2 Quantitative analysis

(1) Initial and final state energies

For analytical and computational convenience, we simplify the soap film into a centrally symmetric, viscous liquid film that deforms in only one direction. A spherical-like droplet of mass m has velocity v and a viscous liquid film with surface tension coefficient σ has no deformation. According to the mechanical energy equation, the initial energy E of the system can be expressed as:

$$E_{\mathrm{i}} = \frac{mv^2}{2}, \tag{1}$$

The end state of this system is shown in Fig. 1, where the viscous liquid film has a vertical morphology of x and a shape similar to a cone; the velocity of the spherical-like droplet at this point is 0 m/s.

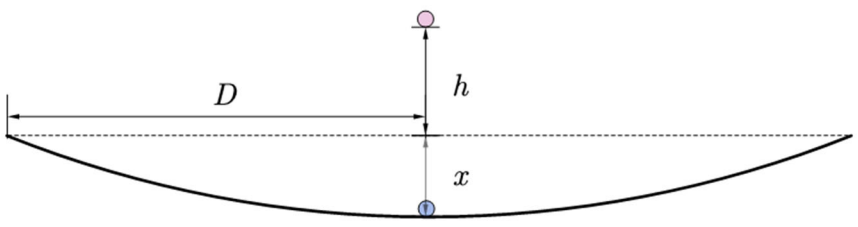

Fig. 1 End-state shape model of a horizontal soap film

According to the surface tension energy equation:

$$E_{\text{surfacetension}} = \sigma \bullet \Delta s, \tag{2}$$

The end-state energy of the system can be obtained by combining the mechanical energy equation,

$$E_{\text{f}} = \sigma\pi D \times \left(\sqrt{x^2 + D^2} - \text{D}\right) - mgx, \tag{3}$$

According to the law of conservation of energy, we have $E_i = E_f$,

$$\frac{mv^2}{2} = \sigma\pi D \times \left(\sqrt{x^2 + D^2} - \text{D}\right) - mgx. \tag{4}$$

Assuming that the density of the spheroidal droplet is ρ, and the radius is r, then the equation (4) can be rewritten as:

$$\frac{2}{3}\rho\pi v^2 r^3 + \frac{4}{3}\rho\pi r^3 gx = \sigma\pi D^2\left(\sqrt{1+\frac{x^2}{y^2}} - 1\right), \tag{5}$$

Since the radius of a spherical-like droplet is much smaller than the radius of a viscous liquid film ($x \ll D$), it follows that:

$$\sigma\pi D^2\left(\sqrt{1+\frac{x^2}{y^2}} - 1\right) = \frac{\sigma\pi x^2}{2}, \tag{6}$$

The equation (5) can then be rewritten as:

$$\frac{2}{3}\rho\pi v^2 r^3 + \frac{4}{3}\rho\pi r^3 gx = \frac{\sigma x^2}{2}, \tag{7}$$

The velocity of the water droplet as it reaches the surface of the soap film is provided by the height at which it falls and the air resistance is negligible. According to the energy conversion equation, equation (7) is equivalent:

$$\frac{4}{3}\rho ghr^3 + \frac{4}{3}\rho r^3 gx = \frac{\sigma x^2}{2}, \tag{8}$$

Since $x \ll h$, the $\frac{4}{3}\rho r^3 gx$ in Eq. can be neglected, we can get:

$$x = \sqrt{\frac{8\rho ghr^3}{3\sigma}}. \tag{9}$$

Also in the case where the concentration of the soap film and the size of the circle are known, its maximum allowable deformation is a fixed value, which we define as x0. From this, if, $x < x0$, the droplet is bounced; if $x > x0$, the droplet penetrates the soap film.

(2) Relationship between angle and drop height

Let us assume that the angle between the soap film and the horizontal is θ (Fig. 2). The expression for x that introduces the angle should be:

$$x = \sqrt{\frac{8\rho ghr^3\cos^2\theta}{3\sigma}}, \tag{10}$$

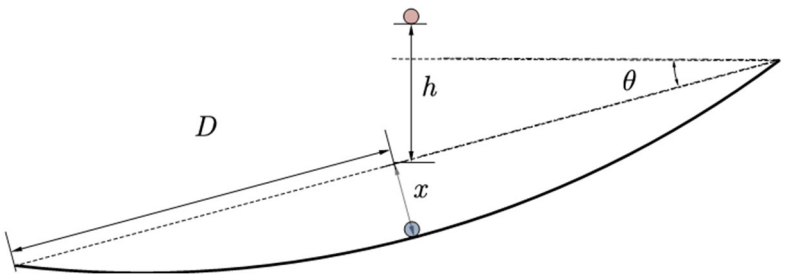

Fig. 2 End-state shape model of a soap film tilted at angle θ

Since x is a constant value, it is derived after a series of derivations:

$$h\cos^2\theta = \frac{3x^2\sigma}{8\rho g r^3}, \tag{11}$$

The relationship between h and θ is shown in Fig. 3:

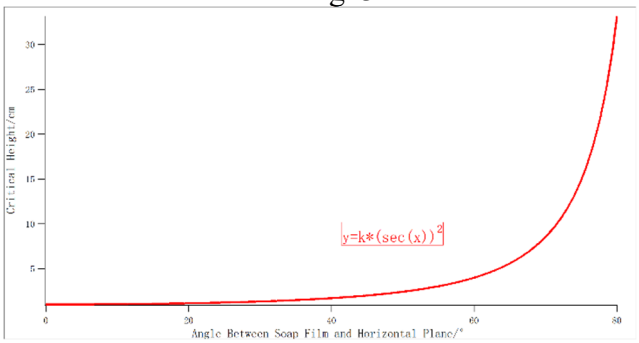

Fig. 3 Image of critical height as a function of the angle between the soap film and the horizontal plane

In Fig. 3, the horizontal coordinate is the tilt angle θ of the soap film and the vertical coordinate is the critical height h, where the scale factor k=3x^2 σ/8ρgr^3. The equation (11) can be rewritten as:

$$\frac{\sqrt{h}}{\sec\theta} = \sqrt{\frac{3x^2\sigma}{8\rho g r^3}}. \tag{12}$$

we can draw the image of $\sqrt{h}$ about $\sec\theta$ should be a straight line with slope $\sqrt{3x^2\sigma/8\rho g r^3}$ (Fig .4).

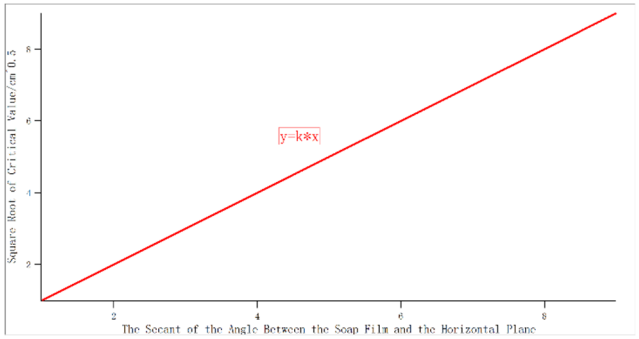

Fig. 4 Image of the square root of the critical height versus the positive cut of the angle between the soap film and the horizontal plane

(3) Relationship between critical height and droplet size

Based on the information that x is constant, we can derive a relationship between the critical height and the droplet size:

$$r^3 = \frac{3\sigma g x^2}{8\rho g h}. \tag{13}$$

Drawing the images of r^3 and1⁄h yields an inverse proportional functional relationship, as shown in Fig. 5:

In Fig. 6, the horizontal coordinate is half of the capillary aperture, i.e., the droplet radius r, and the vertical coordinate is the critical height h, where the scale factor k = (3σx^2)/8ρg. According to equation (13) we can conclude that the graph of the function of h and $r^{1/3}$ should be a straight line.

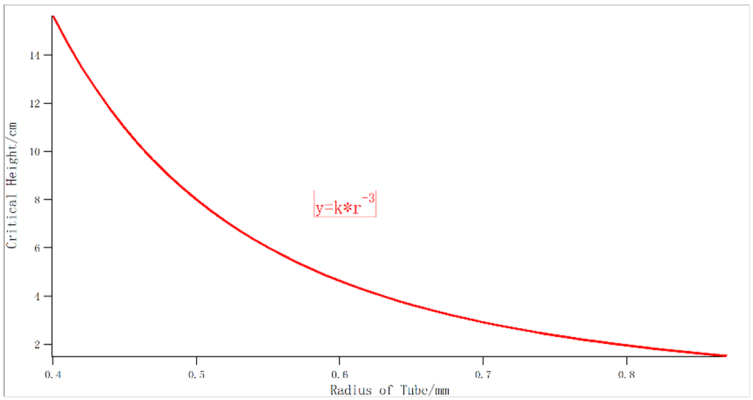

Fig. 5 Image of critical height versus capillary radius

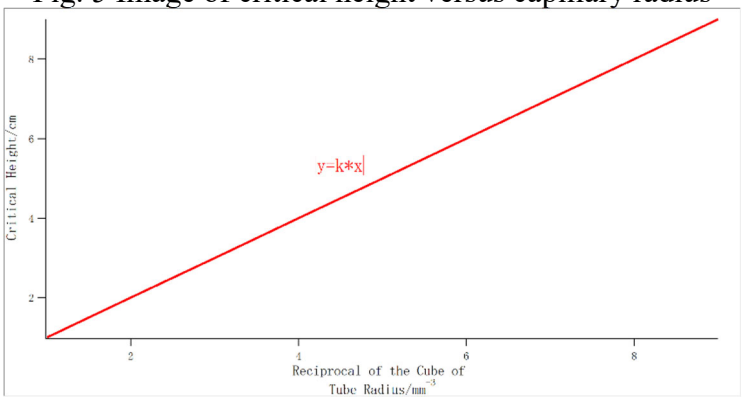

Fig. 6 Plot of critical height vs. -3rd power of capillary radius

(4) Relationship between critical height and suds concentration

According to the existing research on the relationship between surface tension coefficient and concentration of liquid [8], the relationship between surface tension coefficient and concentration of soap water can be approximated as an inverse proportional function, and here, assuming that the concentration of soap water is γ then the relationship equation is:

$$\sigma = \frac{\beta}{a+\gamma}, \tag{14}$$

where α, and β are constant values related to the inverse proportional function relationship. We can derive this by rewriting the expression for x,

$$\sigma = \frac{8\rho g h r^3}{3x^2}, \tag{15}$$

Combining Eq. (14) and (15), we can derive an expression for h as:

$$h = \frac{3\beta x^2}{8\rho g r^3} \bullet \frac{1}{\gamma + a}, \tag{16}$$

That is, h and are inversely proportional to each other, as shown in Fig. 7:

In Fig. 7, the horizontal coordinate is the soap water concentration γ and the vertical coordinate is the critical height h, where:

$$k = \frac{3\beta x^2}{8\rho g}, b = a. \tag{17}$$

In summary, after physical modeling and theoretical analysis, we obtained the relationship between the critical height and the following variables: 1) the larger the tilt angle, the larger the critical height; 2) the larger the concentration of soapy water, the larger the critical height; 3) the larger the droplet, the larger the critical height.

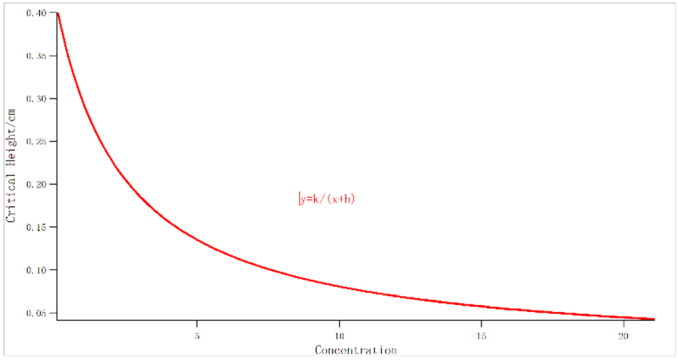

Fig. 7 Image of critical height versus concentration

3. Experiments and Discussions

3.1 Experimental construction

Experimental equipment: iron frame table, wire loop (diameter D = 4.1cm), different sizes of capillary tubes, metal rods, clips, sponges, open box (bottom area and depth are large enough), empty mineral water bottles (volume of about 300mL), scissors, transparent tape, stirring spoon. Ingredients for preparing soapy water: purified water, washing powder, detergent. Camera equipment: cell phone (slow motion photography mode, frame rate of 1600 fps), tripod.

3.2 Experimental operation process

First, we placed the iron frame table smoothly on a horizontal tabletop, fixed the wire loop with a clamp, and fixed it on the iron frame table by a metal bar and tightened the screws. At the same time, we determined the position of the tripod and the height of the stand, and then placed the cell phone for videotaping (Fig. 8).

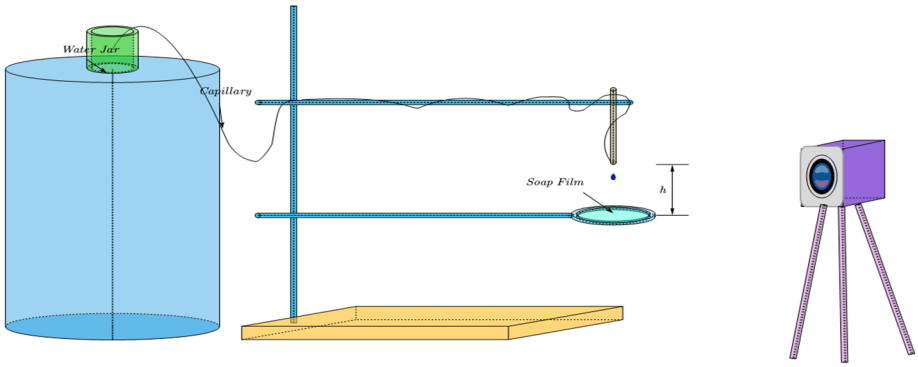

Fig. 8 Schematic diagram of water droplet impact film experiment

Next, we prepared a certain concentration (which will be noted as Concentration A and Concentration B, respectively, in the following) of soapy water, as shown in Table 1. As can be seen from Table 1, concentration B is twice as much as concentration A. We first choose the soap water of concentration A for the experiment.

Table 1 Preparation of different concentrations of soapy water

Material (g)	Concentration A (%)	Concentration B (%)
Purified water	500	500
Laundry detergent	12.78	25.56
Dishwashing liquid	34.94	69.88

3.3 Effect of initial droplet height on the phenomenon of penetration or rebound

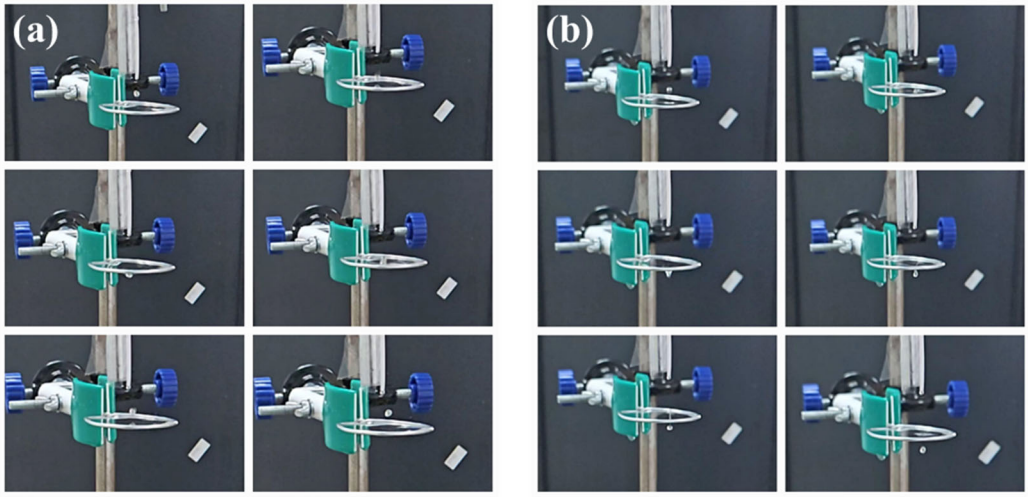

Fig. 9 Pre-experiment. (a) Slow-motion screenshot of a water droplet passing through a soap film and (b) slow-motion screenshot of a water droplet bouncing. (The capillary tubes used in the experiments in the figure were all of 1.6 mm caliber, the concentrations were all of concentration A, and they were all placed horizontally.)

To investigate the effect of the initial height of the water drop on the penetration or rebound phenomenon, we slowly rotate the metal bar holding the wire loop so that the angle between the plane of the loop and the horizontal plane is 0° (the angle can be measured by the phone's own leveling function, and we've verified the accuracy of this tool using a standard protractor). Dip the sponge into the box of soapy water and gently “rub” it in a direction parallel to the plane of the wire loop, which will form a uniform film of soap. At the same time, put one end of the capillary tube into the beaker located in the high place, and the other end is fixed to the soap film directly above the iron bar. Note here that the spout is vertically downward. Then constantly fine-tune the height of the spout, that is, the droplet's initial height of the droplet, we observe the droplet impact on the soap film will appear in three different states: 1) through the soap film (through); 2) into the soap film (critical); 3) by the soap film rebound (rebound) (Fig. 9).

The initial height of the water droplets was recorded, as well as the different states, and the results in Table 2 were obtained for the experimental group with an outer diameter of 1.6 mm, for example:

Table 2 Soap film-droplet interaction versus droplet height for the horizontal case

Interfaces	Soap water concentration	Heights (cm)	Angles	Caliber
Rebound	A	1.2	0	0.8/.16
Boundary	A	1.6	0	0.8/.16
Boundary	A	2	0	0.8/.16
Pass	A	2.4	0	0.8/.16
Pass	A	4	0	0.8/.16
Pass	A	5	0	0.8/.16

After several experiments, we came up with experimental results that were consistent with intuitive expectations. The height at which a droplet falls is positively correlated with the likelihood of penetrating the soap film (within a reasonable error), i.e., the higher the droplet falls, the more it tends to penetrate the soap film; the lower the droplet falls, the more it tends to be rebounded by the soap film, and we refer to the case of an interaction between penetration and rebound as a critical case, and the height of the drop corresponding to such a case as the critical height. The phenomenon is independent of other variables.

3.4 Experiment 1: Relationship between critical height and angle

To investigate the relationship between the critical height and the angle of inclination of the wire loop, we proceeded to vary the angle between the plane of the wire loop and the horizontal plane to

15°, 30°, and 45° in that order (Fig. 10). In all three sets of experiments, we used capillary tubes with a caliber of 1.6 mm, soapy water of concentration A and the same height. It can be found that the change in the angle of inclination causes a change in the interaction state of the water droplets with the film at the same height. The experimental data are shown in Table 3 below, where heights 1-3 correspond to the drop heights at angles 0, 15, and 30 degrees, respectively.

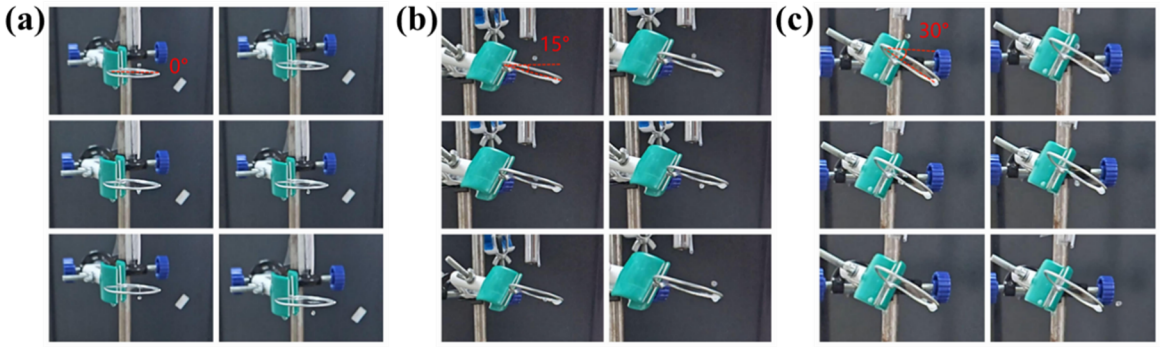

Fig. 10 Adjustment of the tilt angle of the wire loop. (a) Water droplets pass through the soap film at a tilt angle of 0 degrees; (b) droplets bounce at a tilt angle of 15 degrees; (c) droplets bounce at a tilt angle of 30 degrees

Table 3 Soap film-droplet interactions at different angles and heights using a 1.6 aperture capillary at concentration A

Interfaces	Heights 1 (cm)	Interfaces	Heights 2 (cm)	Interfaces	Heights 3 (cm)	Interfaces	Heights 4 (cm)
Rebound	1.2	Rebound	1.3	Rebound	1.7	Rebound	2
Boundary	1.6	Rebound	1.6	Boundary	2	Rebound	2.5
Boundary	2	Boundary	1.8	Boundary	2.6	Boundary	3
Pass	2.4	Boundary	2.2	Pass	3	Boundary	3.5
Pass	4	Pass	2.6	Pass	4	Boundary	4
Pass	6	Pass	4	Pass	7	Pass	4.3

In discussing only the critical case, continuing to rely on Eq. 12, we can obtain Fig. 11. The results of our fit show that the graph is a straight line, in line with the conclusions of previous theoretical projections

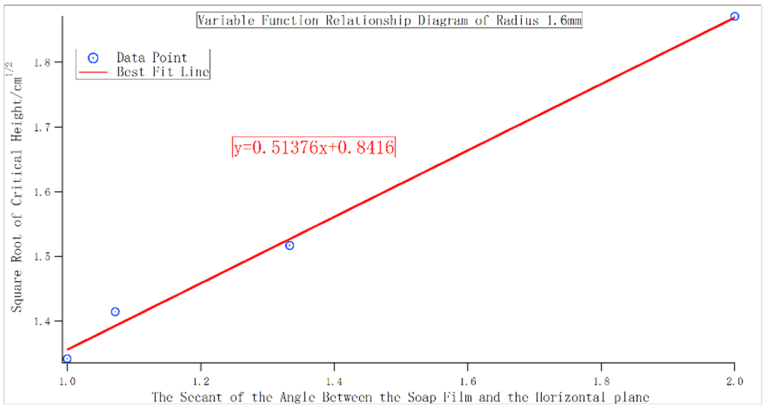

Fig. 11 Experimental data plot of the square root of the critical height versus the orthogonal cut of the angle between the soap film and the horizontal plane

3.5 Experiment 2: Relationship between critical height and droplet size

There are four sizes of capillary tubes in this experiment: 0.6 mm, 0.9 mm, 1.2 mm, and 1.6 mm (Fig. 12). Similarly, the capillary tube with a diameter of 1.6mm was used for the experiment, and one end of the capillary tube was glued to the end of a metal rod with transparent tape, leaving a

length of about 4mm on the outside, and the rod was fastened to a metal stand and screwed tightly. The other end of the capillary tube is submerged in a bottle of soapy water, making sure that the height of this end is higher than that of the end glued to the metal rod (the spout). According to the principle of siphoning, the spout will drop drops of soapy water at a steady frequency, and the four calibers we chose ensure that this frequency is moderate, neither too fast nor too slow. Next, we adjusted the position of the metal rods on the iron stand so that the droplets would come out of the spout and fall to the center of the wire loop. Since the diameter of the capillary tube is proportional to the radius of the drop, changing the capillary tube is essentially changing the drop size. Based on the above experiments, the following experimental results were obtained in Table 4, where heights 1-3 corresponded to capillary calibers of 1.6, 1.4, 1.2, and 0.9 mm, respectively.

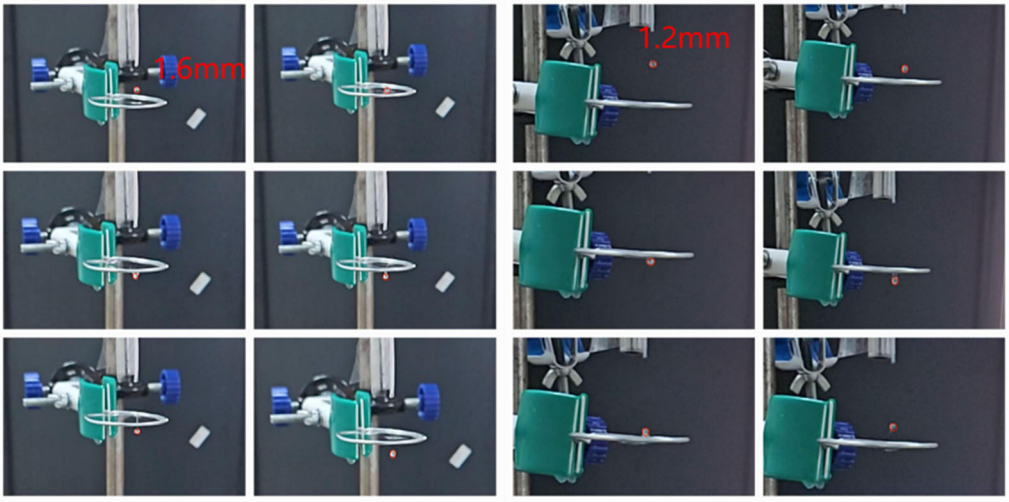

Fig. 12 An illustration of the droplet size setting

Table 4 Interaction of droplets with soap film at different pore sizes and heights

Interfaces	Heights 1 (cm)	Interfaces	Heights 2 (cm)	Interfaces	Heights 3 (cm)	Interfaces	Heights 4 (cm)
Rebound	1.2	Rebound	2	Rebound	1.3	Rebound	1
Boundary	1.6	Rebound	2.3	Boundary	1.6	Boundary	1.5
Boundary	2	Boundary	2.6	Boundary	1.8	Boundary	1.7
Pass	2.4	Boundary	3	Boundary	2	Boundary	2
Pass	4	Boundary	3.2	Boundary	2.8	Boundary	2.4
Pass	6	Pass	3.5	Pass	3.1	Pass	2.8
Rebound	2	Pass	4	Pass	5	Pass	4

Again, we focus solely on the critical height case and plot the function of r3 alongside its inverse function based on the previously derived equation (13) (Fig. 13). It is easy to see that the two are positively correlated, in line with the conclusions of previous theoretical projections.

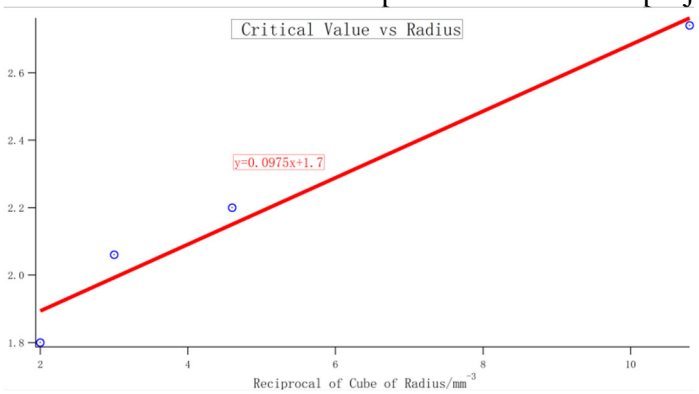

Fig. 13 Experimental data plot of critical height versus -3rd power of capillary aperture

3.6 Experiment 3: Relationship between critical height and suds concentration

When experiments three and four were completed, we finally changed the concentration of the soapy water so that it was divided into concentrations A and B. At this point, we only used capillary tubes with a caliber of 0.9 mm for the experiment and made sure that the plane of the wire loop was horizontal (i.e., the angle was equal to 0°), controlling for these variables to remain constant. After this complete process, we successfully changed four variables: height, angle, concentration, and caliber. This is the basic framework of our controlled variable experiment. The experimental data are shown in Table 5. Here we still discuss only the critical height, and according to the previously obtained Eq. 16, we know that the critical height is inversely proportional to the concentration, i.e., the graph of the function of h and γ is plotted as an approximate inverse proportional function image (Fig. 14).

Table 5 Interaction of droplets with soap film at different concentrations

Interfaces	Concentration A (cm)	Interfaces	Concentration A (cm)
Rebound	2	Rebound	1.6
Boundary	2.3	Boundary	1.9
Boundary	2.6	Boundary	2.2
Boundary	3	Boundary	2.4
Boundary	3.2	Boundary	2.8
Pass	3.5	Pass	3
Pass	4	Pass	2.5

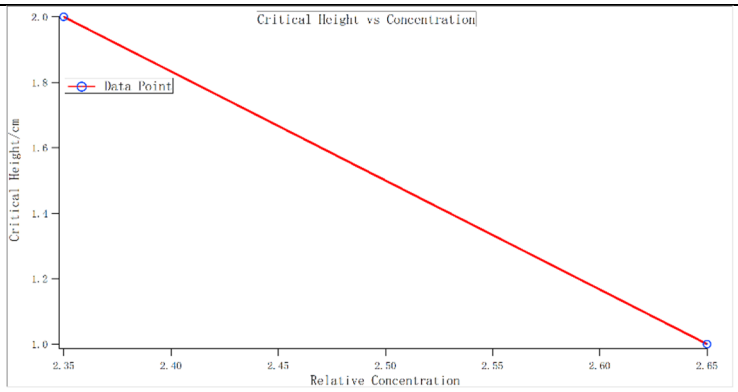

Fig. 14 Experimental data plot of critical height versus suds concentration

3.7 Discussion

We succeeded in observing three phenomena during the experiment: pass-through, incorporation, and rebound, and we made sure that each phenomenon occurred enough times under different conditions to indicate the non-accidental nature of the experimental phenomena. Furthermore, because all of the variable conditions that can cause a droplet to incorporate into a soap film can also cause a droplet to bounce off of a soap film, we decided to combine these two phenomena into a failure to pass through a soap film, and the dependent variable that we wanted to investigate: the critical height, is the approximate boundary that delineates whether a droplet can pass through a soap film (because systematic error dictates that this boundary cannot be very precise, we use the term “approximate boundary"). The experimental phenomena show that each independent variable affects the dependent variable, with the tilt angle being positively correlated with the critical height, the droplet size being negatively correlated with the critical height, and the suds concentration being positively correlated with the critical height.

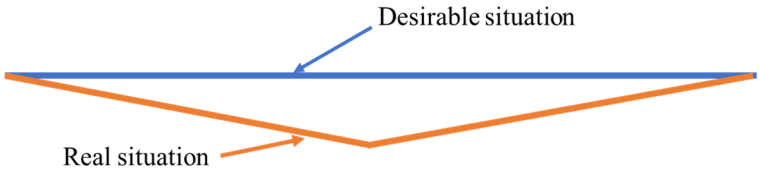

Fig. 15 Realistic soap film thickness

In the experiment, when we change the tilt angle of the soap film, the thickness of the soap film is not uniform due to gravity, in this paper we ignore this phenomenon for the consideration of simplifying the model, and through the experiment we also prove that the unevenness of the thickness does not significantly affect the experimental results (Fig. 15). During Experiment 1, we disregarded the shaping effect of the droplet's component in the direction parallel to the soap film on the soap film morphology and ignored the energy loss due to viscous drag during the sliding of the droplet on the soap film surface (Fig. 16).

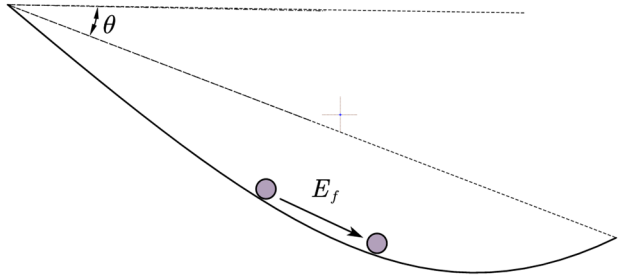

Fig. 16 Schematic illustration of the actual shape of the soap film and the energy loss to the droplets by the drag force

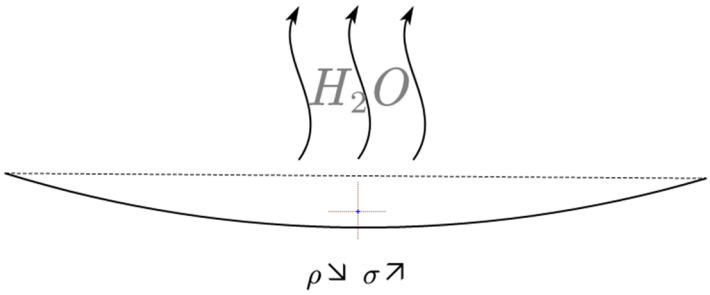

Fig. 17 The slow evaporation of soap water causes small changes in the density and surface tension coefficient of the soap film

The surface tension of the soap film in the experiment decreases slowly over time due to the slow evaporation of the soapy water, but we do not consider the effect of the length of time the soap film has been present on its physical properties in our data processing (Fig. 17). The soap film was not completely horizontal in its initial state, but had a very slight natural droop, but we ignored this confounding factor, considering that its shape variable was much smaller than the minimum shape variable that would allow a droplet to pass through it. In addition, the radius of the wire loop is an independent variable that could have affected the critical height and altered the experimental phenomenon, but we did not specifically discuss the effect of this variable for time reasons.

4. Summary

Focusing on the interaction between droplets and soap film, this study systematically investigates the penetration and rebound behavior of droplets on the surface of soap film by building a professional experimental setup. Based on the law of energy conservation, a refined physical model was constructed to quantitatively analyze the relationship between key parameters—such as initial droplet height, angle of incidence, soap solution concentration, and droplet size—and the droplet's motion state on the soap film surface. In the research process, firstly, the principle of controlling variables was strictly followed to design and carry out several groups of controlled experiments, and high-precision measuring equipment was used to collect data to ensure the accuracy and reliability of the experimental results; secondly, the quantitative theoretical model constructed was repeatedly verified and optimized, and the prediction results were highly compatible with the experimental data, which

effectively revealed the intrinsic law of the interaction between the droplets and the soap film; and it was found that the relationship between the droplet characteristic height (h) and the droplet size (h) was very close. The characteristic droplet height (h) is significantly inversely proportional to the surface tension (γ), the square root of the height ($\sqrt{h}$) is proportional to the incidence angle secant ($\sec\theta$), and the height (h) is inversely proportional to the third power of the droplet radius (r^3), and these conclusions provide an important theoretical basis for the research in this field.

In the future, the research will be deepened and expanded from three dimensions: first, to explore more potential influence parameters and improve the theoretical system of the interaction mechanism; second, to conduct full-flow numerical simulation using COMSOL software to accurately analyze the deformation process of the soap film under the effect of gravity; and third, to explore the potential of this phenomenon for application in the fields of life sciences and biotechnology, and to promote the transformation of theoretical results into practical applications to facilitate the innovative development of the related technologies. Third, we will explore the potential applications of this phenomenon in life sciences, biotechnology, and other fields, promote the transformation of theoretical results into practical applications, and facilitate the innovative development of related technologies [9, 10].

References

[1] Taylor, Jean E. "The structure of singularities in soap-bubble-like and soap-film-like minimal surfaces." Annals of Mathematics 103. 3(197): 489-539.

[2] Courant, Richard. "Soap film experiments with minimal surfaces." The American Mathematical Monthly 47.3 (1940): 167-174.

[3] Ruckenstein, Eli, and Rakesh K. Jain. "Spontaneous rupture of thin liquid films." Wetting Theory. CRC Press, 2018. 588-603.

[4] Gilet, Tristan, and John WM Bush. "The fluid trampoline: droplets bouncing on a soap film." Journal of Fluid Mechanics 625 (2009): 167-203.

[5] Chen, C.-H., et al. "The distortion of a horizontal soap film due to the impact of a falling sphere." Chemical Engineering Science 206(2019): 305-314.

[6] Culick, Fred EC. "Comments on a ruptured soap film."Journal of Applied Physics 31.6(1960): 1128-1129.

[7] Basu, Saikat, et al. "On angled bounce-off impact of a drop impinging on a flowing soap film." Fluid Dynamics Research 49.6(2017): 065509.

[8] Cheng J, Li L, Liu K. Study on the relationship between liquid surface tension and concentration (In Chinese). China Measurement & Test, 2014, 40(3): 32-34.

[9] Buguin, A., Y. Chen, and P.Silberzan. "Microfluidics: Concepts and applications to the life sciences." Nanoscience: Nanobiotechnology and Nanobiology(2009): 743-774.

[10] Javadi, Arman, et al. "Effect of wetting on capillary pumping in microchannels." Scientific Reports 3.1 (2013): 1412